Dioxygen Activation by a Macrocyclic Copper Complex Leads to a Cu₂O₂ Core with Unexpected Structure and Reactivity

Dr. Isaac Garcia-Bosch[a], **Dr. Ryan E. Cowley**[b], **Daniel E. Díaz**[c], **Maxime A. Siegler**[c], **Prof. Wonwoo Nam**[d], **Prof. Edward I. Solomon**[b], and **Prof. Kenneth D. Karlin**[c]

Isaac Garcia-Bosch: igarciabosch@smu.edu; Wonwoo Nam: wwnam@ewha.ac.kr; Edward I. Solomon: edward.solomon@stanford.edu; Kenneth D. Karlin: karlin@jhu.edu

[a]Department of Chemistry, Southern Methodist University, Dallas, Texas 75275 (United States)

[b]Department of Chemistry, Stanford University, Stanford, California 94305 (United States)

[c]Department of Chemistry, Johns Hopkins University, Baltimore, Maryland 21218 (United States)

[d]Department of Chemistry and Nano Science, Ewha Womans University, Seoul 120–750 (Korea)

Abstract

We report the Cu^I/O_2 chemistry of complexes derived from the macrocylic ligands 14-TMC (1,4,8,11-tetramethyl-1,4,8,11-tetraazacyclotetradecane) and 12-TMC (1,4,7,10-tetramethyl-1,4,7,10-tetraazacyclododecane). While $[(14\text{-TMC})Cu^I]^+$ is unreactive towards dioxygen, the smaller analog $[(12\text{-TMC})Cu^I(CH_3CN)]^+$ reacts with O_2 to give a side-on bound peroxo-dicopper(II) species (^{S}P), confirmed by spectroscopic and computational methods. Intriguingly, 12-TMC as a N4 donor ligand generates ^{S}P species, thus in contrast with the previous observation that such species are generated by N2 and N3 ligands. In addition, the reactivity of this macrocyclic side-on peroxodicopper(II) differs from typical ^{S}P species, because it reacts only with acid to release H_2O_2, in contrast with the classic reactivity of Cu_2O_2 cores. Kinetics and computations are consistent with a protonation mechanism whereby the TMC acts as a hemilabile ligand and shuttles H^+ to an isomerized peroxo core.

Keywords

bioinorganic chemistry; copper; dioxygen reduction; macrocyclic ligands; metal–peroxo complexes

---

Over the last 3 decades, our research interests have included a focus on the study of transient species derived from the reaction between Cu^I complexes with dioxygen.[1] Rational design of the ligand employed has allowed our group, among others,[2] to extensively characterize the formation of mononuclear[3] and dinuclear[4] copper–dioxygen assemblies (Figure 1A). Many of our findings are based on the tripodal ligand TMPA (tris((2-pyridyl)methyl)amine) and its derivatives, that have allowed fine tuning of the electronic and steric properties of

Cu/O_2 derived species.[5] Particularly relevant are our recent findings in the stabilization of mononuclear end-on $LCu^{II}(O_2^{\bullet-})$ species (**E**S) making use of electron-rich TMPA derivatives[6] or by H-bonding interactions,[7] and our recent reports on the first examples of end-on peroxo-dicopper(II) intermediates (**E**P) that undergo reversible O–O cleavage via formation of dicopper(III) bis(μ-oxo) species (**O**).[8] These results show that even after many years of study, new Cu/O_2 reactivity patterns are still emerging.

One of the most extensively employed ligand types in bioinspired O_2-activation chemistry is the macrocycle 14-tetramethylcyclam (14-TMC), along with its contracted analogue 12-TMC. Nam and co-workers have extensively characterized M-($O_2^{\bullet-}$) and M-($O_2(H)$) complexes of the 1st row of transition metals (Figure 1B); associated O_2 activation levels and substrate reactivity are dependent on both metal identity and TMC ring size.[9] However, the reactivity of analogous TMC/Cu/O_2 systems has remained elusive. Schindler and co-workers[10] recently reported the first example of end-on peroxo Cu_2O_2 species (**E**P) bearing a macrocyclic ligand *tetb* (*rac*-5,5,7,12,12,14-hexamethyl-1,4,8,11-tetraazacyclotetradecane), a **E**P complex with a distorted square-pyramidal (τ = 0.3) geometry and equatorial bound bent bridging O_2^{2-} ligand (Figure 1C). This geometry differs from the TMPA-based **E**P species, where the O_2^{2-} ligand is found to be coordinated in an axial position of a trigonal bipyramidal (τ = 0.9)[11] geometry (Figure 1C), and suggests macrocyclic ancillary ligands can form Cu/O_2 species with unique structure. Herein, we report the first study on the Cu–O_2 chemistry of the 14-TMC and 12-TMC systems and the first example of a side-on (i.e., μ-η^2:η^2) peroxodicopper(II) complex (**S**P) bearing the 12-TMC ligand.

Mixing equimolar amounts of the 14-TMC ligand with $[Cu^I(CH_3CN)_4](BAr^F)$ (BAr^F: $B(C_6F_5)_4^-$) in Et_2O at room temperature under Ar allows the growth of colorless crystals, which were analyzed by single crystal X-ray diffraction (Figure 2A); the 14-TMC ligand shows an unusual type-*V* (*TV*) conformation (*TV*, where 1,8-Me groups are oriented up; 4,11-Me groups down)[12] in the Cu^I complex *TV*-$[(14\text{-TMC})Cu^I]^+$,[13] where the Cu ion adopts a flattened tetrahedral geometry. Surprisingly, this macrocyclic type-V $[(14\text{-}TMC)Cu^I]^+$ complex is completely unreactive towards O_2 (see the Supporting Information for details).[14]

The 12-TMC cuprous complex was synthesized similarly and the X-ray structural determination disclosed an $N_5Cu(I)$ center in which the 12-TMC ligand adopts a type-*I* conformation (with all Me groups up) in *TI*-$[(12\text{-TMC})Cu^I(CH_3CN)](BAr^F)$ with a tightly coordinated acetonitrile molecule (d(Cu-N_{CH3CN}) = 1.92 Å) (Figure 2B). Unlike for *TV*-$[(14\text{-TMC})Cu^I]^+$, *TI*-$[(12\text{-TMC})Cu^I(CH_3\text{-}CN)]^+$ reacts with O_2 at −90 to −135 °C, forming a new green species in acetone or MeTHF (2-methyltetrahydrofuran). UV/Vis spectroscopy (Figure 3A) reveals an intense high-energy spectral feature at 364 nm (ε = 20 m$_M^{-1}$ cm^{-1}) and two weak transitions at 450 and 635 nm, which are characteristic of a complex with a side-on peroxodicopper(II) coordination (**S**P).[2a] $[(12\text{-TMC})_2Cu^{II}_2(O_2^{2-})]^{2+}$ is the first example of a **S**P complex bearing a tetradentate ligand; N_4 ligands typically provide for an end-on peroxo (**E**P) coordination.

Additional proof for the side-on $[(12\text{-TMC})_2Cu^{II}_2(O_2^{2-})]^{2+}$ formulation is provided by resonance Raman (rR) spectroscopy (Figure 3A, inset). Laser excitation (λ = 380 nm) of

frozen samples of $[(12\text{-TMC})_2Cu^{II}_2(O_2^{2-})]^{2+}$ generated in both MeTHF and acetone led to observation of an isotope-sensitive feature at $\nu_{Cu-O} = 544$ cm^{-1} ($(^{18}O_2) = -29$ cm^{-1}) plus a $\nu_{Cu-Cu} = 264$ cm^{-1} isotope-insensitive feature that are typical of ^{S}P complexes.[15] Higher energy features are observed at 1085 cm^{-1} and around 1340 cm^{-1}, and are consistent with assignments as an overtone ($2\nu_{Cu-O}$) and combination band ($2\nu_{Cu-O}+\nu_{Cu-Cu}$), respectively. Since the antisymmetric ν_{Cu-O} mode is not Raman active in a planar core, the unusually high intensity of ν_{Cu-O} in $[(12\text{-TMC})_2Cu^{II}_2(O_2^{2-})]^{2+}$ suggests the Cu_2O_2 core adopts a butterfly-distorted geometry (see below). This is consistent with the perpendicular $\pi^*_v \rightarrow Cu$ LMCT being observed (450 nm), which is a feature that has no intensity in planar $Cu_2(O_2^{2-})$ cores.[15b]

DFT calculations of the $[(12\text{-TMC})_2Cu^{II}_2(O_2^{2-})]^{2+}$ intermediate led to the ^{S}P species as the lowest energy isomer, with both Cu centers presenting a distorted octahedral geometry around a butterflied Cu_2O_2 core (Figure 3 B), as suggested by the experimental UV/Vis and rR spectroscopies.[16] The calculated Cu–O, O–O and Cu–Cu distances are consistent with other well-characterized ^{S}P complexes.[17] The optimized Cu–N$_{av}$ distance (2.32 Å) was found to be slightly longer than the ones found for other ^{S}P-type species (2.0–2.2 Å), due to the elongation of two of the Cu–N distances per Cu ion (2.39–2.56 Å). These weak Cu–N bonds have also been observed by Tolman and co-workers in the Cu/O_2 species bearing tridentate macrocyclic systems, inducing the formation of O-type species over ^{S}P.[18] In our case, we propose that these weak, pseudoaxial, Cu–N bonds are a key factor to explain the unusual reactivity of the macrocyclic ^{S}P core (vide infra). DFT and TD-DFT calculations also reproduce the experimental rR data (calcd $\nu_{Cu-O} = 514$ cm^{-1} [exptl: 544 cm^{-1}]; calcd $\nu_{Cu-Cu} = 268$ cm^{-1} (exptl: 264 cm^{-1}); and absorption spectrum (calcd: 351, 450 and 622 nm; exptl: 364, 450 and 635 nm, see Figure S9).

The study of the reactivity of the different Cu_2O_2 centers ($^{E}P, ^{S}P, O$) towards external substrates has led to some general rules which depend on the core formulation.[19] ^{E}P complexes are considered basic/nucleophilic species, while ^{S}P and O-type complexes are considered non-basic/electrophilic.[19] However, this ^{S}P $[(12\text{-TMC})_2Cu^{II}_2(O_2^{2-})]^{2+}$ species is found to be unreactive towards external substrates usually oxidized by electrophilic species (Figure 4A): phenols (2,4-tBu$_2$-PhOH/2,6-tBu$_2$-4-MeO-PhOH, for H$^\bullet$ abstraction), sodium phenolates (for *ortho*-hydroxylation) and PPh$_3$ (for O-atom transfer) are each unreactive when added in excess (up to 50 equiv, see SI). The 12-TMC-based ^{S}P species is also found to be stable when it was exposed to substrates that can be oxidized by nucleophilic $M(O_2^{2-})$ species such as 4-substituted benzaldehydes (oxidation to benzoic acids) or cyclohexanecarboxaldehyde (decarboxylation to cyclohexene).[9a]

On the other hand, when $[(12\text{-TMC})_2Cu^{II}_2(O_2^{2-})]^{2+}$ was exposed to a strong acid (H$^+\bullet$DMF$\bullet$CF$_3$SO$_3^-$), decay of its UV/Vis features was observed (Figure 4B) with concomitant formation of new weak features centered at 590 nm, corresponding to the mononuclear $[(12\text{-TMC})Cu^{II}(L)]^{2+}$ complex (for Cu^{II} quantification and EPR characterization see Figure S7). H$_2$O$_2$ formation was confirmed by iodometric titration of the final reaction solution (95% based on $[Cu_2O_2]_0$, see Figure S6). To the best of our knowledge, this is one of the first examples of a ^{S}P species that can be protonated quantitatively to release H$_2$O$_2$, a reaction that is typical of ^{E}P complexes.[20]

In order to obtain mechanistic insight, kinetic analysis on the reaction of [(12-TMC)$_2$Cu$^{II}_2$(O$_2^{2-}$)]$^{2+}$ with (H$^+$•DMF•CF$_3$SO$_3^-$) was conducted under pseudo-first-order conditions (5–20 equiv of acid). The decrease of the ^{S}P UV/Vis features over time was fit using pseudo-first-order exponential decays to obtain the kinetic constants (k_{obs}) at different [H$^+$] (Figure 4B, inset). The k_{obs} increased parabolically with increasing acid concentration (rate law: d[Cu$_2$O$_2$]/$dt = -k_{H+}$[Cu$_2$O$_2$][H$^+$]^2), suggesting an unusual involvement of 2 molecules of acid during the rate determining step (r.d.s.). The same kinetic behavior was observed with mild acids such as substituted acetic acids (RCO$_2$H, R: Cl$_3$C, Cl$_2$HC, CF$_3$, CH$_3$). The k_{obs} values were found to be independent on the H$^+$ strength and an inverse kinetic isotope effect (KIE) was observed ($k_{CF3CO2H}/k_{CF3CO2D}$ = 0.8, see Figure S5 in the Supporting Information).

Protonation of Cu$_2$O$_2$ species to generate H$_2$O$_2$ is characteristic of ^{E}P species; ^{S}P cores are usually stable under acidic conditions. However, the basicity of this [(12-TMC)$_2$Cu$^{II}_2$(O$_2^{2-}$)]$^{2+}$ complex is not matched with a nucleophilic character. We propose that the unique reactivity of [(12-TMC)$_2$Cu$^{II}_2$(O$_2^{2-}$)]$^{2+}$ is dictated by the ligand, since the 6-coordinate Cu ions have no coordination positions available in the Cu$_2$O$_2$ core for incoming substrates. The lack of a pK_a effect in the O$_2^{2-}$ protonation indicates the r.d.s. involves protonation by a common intermediate, regardless of the identity of added acid. This suggests the TMC ligand is initially protonated by acid, and subsequently transfers H$^+$ intramolecularly to the peroxide. DFT calculations support this idea, showing that two sequential TMC protonation events lead first to isomerization of the ^{S}P to a mono-protonated η$_2$:η^1-Cu$_2$O$_2$ and subsequently a di-protonated ^{E}P species (Figure 5), both stabilized by H-bonding interactions. We propose that this nucleophilic ^{E}P core is now activated towards intramolecular H$^+$ transfer from the protonated N atoms of TMC (see Figures S10–S13 in the Supporting Information).

The experimental observations (2nd order in [H$^+$] with no pK_a effect) and DFT calculations point towards a mechanism where a first fast protonation to 12-TMC (uphill)[21], enabled by the weak Cu–N bonds, is followed by a second rate-determining protonation. Rate-limiting proton transfer from 12-TMC to the peroxo moiety is also consistent with the inverse KIE since the O–H bond being formed is stronger than the N–H bond being broken. We propose that the macrocyclic ligand has a dual role upon protonation: the flexibility to accommodate different Cu$_2$O$_2$ isomers (control of the primary coordination sphere) and the ability to act as a proton shuttle (control of the secondary coordination sphere by H-bonding interactions). A similar duality is observed in the reactivity of selected metalloenzymes (e.g. Cu,Zn-SOD[22]) and bio-inspired catalysts (e.g. Ni-catalyzed H$_2$ formation[23]).

In conclusion, we have succeeded in generating and describing previously elusive LCu/O$_2$ chemistry of the macrocyclic ligands 14-TMC and 12-TMC. The dramatic effects on structure and chemistry previously known for differing TMC ring-size,[9] along with the finding of a 12-TMC Cu^I/O$_2$ adduct with distinctive structure and behavior, are manifest by the new findings. Current studies are focused on understanding the Cu-dioxygen chemistry of other TMC isomers generated in the in situ reactions of 14-TMC/Cu^I,[14a] along with exploring other macrocyclic systems beyond 12-TMC and 14-TMC likely to provide Cu/O$_2$ derived species with new structural, spectroscopic and reactivity features.

Supplementary Material

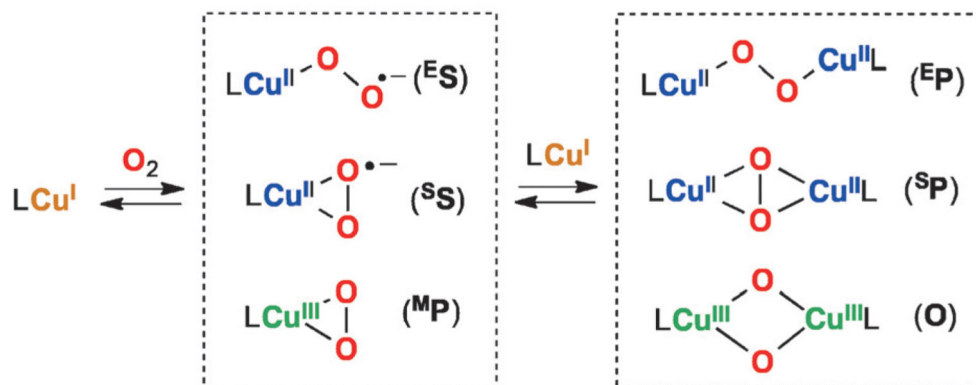Refer to Web version on PubMed Central for supplementary material.
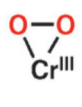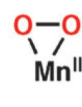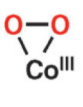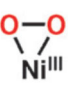
Acknowledgments

References
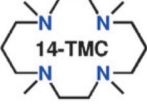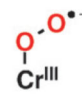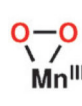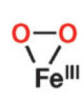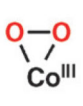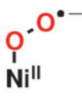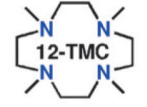
1. a) Himes RA, Karlin KD. Curr. Opin. Chem. Biol. 2009; 13:119–131. [PubMed: 19286415] b) Hatcher LQ, Karlin KD. Adv. Inorg. Chem. 2006; 58:131–184.

2. a) Mirica LM, Ottenwaelder X, Stack TDP. Chem. Rev. 2004; 104:1013–1045. [PubMed: 14871148] b) Lewis EA, Tolman WB. Chem. Rev. 2004; 104:1047–1076. [PubMed: 14871149]

3. a) Aboelella NW, Lewis EA, Reynolds AM, Brennessel WW, Cramer CJ, Tolman WB. J. Am. Chem. Soc. 2002; 124:10660–10661. [PubMed: 12207513] b) Fujisawa K, Tanaka M, Morooka Y, Kitajima N. J. Am. Chem. Soc. 1994; 116:12079–12080.

4. a) Halfen JA, Mahapatra S, Wilkinson EC, Kaderli S, Young VG Jr, Que L Jr, Zuberbühler AD, Tolman WB. Science. 1996; 271:1397–1400. [PubMed: 8596910] b) Mirica LM, Vance M, Rudd DJ, Hedman B, Hodgson KO, Solomon EI, Stack TDP. Science. 2005; 308:1890–1892. [PubMed: 15976297]

5. a) Jacobson RR, Tyeklár Z, Karlin KD, Liu S, Zubieta J. J. Am. Chem. Soc. 1988; 110:3690–3692.b) Zhang CX, Kaderli S, Costas M, Kim E-i, Neuhold Y-M, Karlin KD, Zuberbühler AD. Inorg. Chem. 2003; 42:1807–1824. [PubMed: 12639113]

6. Lee JY, Peterson RL, Ohkubo K, Garcia-Bosch I, Himes RA, Woertink J, Moore CD, Solomon EI, Fukuzumi S, Karlin KD. J. Am Chem. Soc. 2014; 136:9925–9937. [PubMed: 24953129]

7. Peterson RL, Himes RA, Kotani H, Suenobu T, Tian L, Siegler MA, Solomon EI, Fukuzumi S, Karlin KD. J. Am. Chem. Soc. 2011; 133:1702–1705. [PubMed: 21265534]

8. a) Kieber-Emmons MT, Ginsbach JW, Wick PK, Lucas HR, Helton ME, Lucchese B, Suzuki M, Zuberbühler AD, Karlin KD, Solomon EI. Angew Chem. Int. Ed. 2014; 126:5035–5039.b) Kim S, Ginsbach JW, Billah AI, Siegler MA, Moore CD, Solomon EI, Karlin KD. J. Am. Chem. Soc. 2014; 136:8063–8071. [PubMed: 24854766]

9. a) Cho J, Sarangi R, Nam W. Acc. Chem. Res. 2012; 45:1321–1330. [PubMed: 22612523] b) Rohde J-U, In J-H, Lim MH, Brennessel WW, Bukowski MR, Stubna A, Münck E, Nam W, Que L Jr. Science. 2003; 299:1037–1039. [PubMed: 12586936] c) Ray K, Pfaff FF, Wang B, Nam W. J. Am. Chem. Soc. 2014; 136:13942–13958. [PubMed: 25215462]

10. Hoppe T, Schaub S, Becker J, Würtele C, Schindler S. Angew. Chem. Int. Ed. 2013; 52:870–873. *Angew. Chem.* **2013,** *125,* 904–907.

11.

For square-pyramidal ($\tau = 0$) and trigonal bypyramidal ($\tau = 1$) geometry analysis described by: Addison AW, Rao TN, Reedijk J, van Rijn J, Verschoor GC. J. Chem. Soc., Dalton Trans. 1984:1349–1356.

12. Bosnich B, Poon CK, Tobe M. Inog. Chem. 1965; 4:1102–1108.

13.

Cyclic voltammetry experiments using TV-[(14-TMC)Cu^I](BAr^F) as starting material matched the 1 e– redox behavior ($E^0 = -0.36$ V vs. Fc$^{+/0}$) of the unidentified 14-TMC/Cu^I product observed in previous electrochemical studies (see the Supporting Information). Bucher C, Duval E, Espinosa E, Barbe J-M, Verpeaux J-N, Amatore C, Guilard R. Eur. J. Inorg. Chem. 2001:1077–1079.

14.

a) Current experiments are carried out where in situ generation of other than type-V 14-TMC/Cu[I] isomers leads to new 14-TMC/Cu/O_2 derived species. These results will be published elsewhere. b) CCDC 1446257, 1446258, and 1446259 contain the supplementary crystallographic data for this paper. These data are provided free of charge by The Cambridge Crystallographic Data Centre.

15.

The $\nu(O–O)$ was not observed by rR, however the $\nu(Cu–O)$ and $\nu(Cu–Cu)$ belong unambiguously to a SP species: Henson MJ, Vance MA, Zhang CX, Liang H-C, Karlin KD, Solomon EI. J. Am. Chem. Soc. 2003; 125:5186–5192. [PubMed: 12708870] Pidcock E, Obias HV, Abe M, Liang H-C, Karlin KD, Solomon EI. J. Am. Chem. Soc. 1999; 121:1299–1308.

16.

Karlin KD, Tyeklár Z, Farooq A, Haka MS, Ghosh P, Cruse RW, Gultneh Y, Hayes JC, Toscano PJ, Zubieta J. Inorg. Chem. 1992; 31:1436–1451. b) The DFT optimized structure of the **SP** complex where the 12-TMC ligand is acting as a tridentate ligand was found to be 16 kcal mol^{-1} higher in energy.

17. Kodera M, Katayama K, Tachi Y, Kano K, Hirota S, Fujinami S, Suzuki M. J. Am. Chem. Soc. 1999; 121:11006–11007.

18. Lam BMT, Halfen JA, Young VG Jr, Hagadorn JR, Holland PL, Lledos A, Cucurull-Sanchez L, Novoa JJ, Alvarez S, Tolman WB. Inorg. Chem. 2000; 39:4059–4072. [PubMed: 11198861]

19. Paul PP, Tyeklár Z, Jacobson RR, Karlin KD. J. Am. Chem. Soc. 1991; 113:5322–5332.

20. Santagostini L, Gullotti M, Monzani E, Casella L, Dillinger R, Tuczek F. Chem. Eur. J. 2000; 6:519–522. [PubMed: 10747419]

21.

a) A mechanistic scenario where a concerted diprotonation of the Cu_2O_2 center is also plausible. Additional studies are necessary to distinguish between these two reaction pathways. b) The inverse KIE indicates the N–H/O–H bonding interaction at the TS is stronger than the N–H bond in the reactant. This is consistent with the higher frequency O-H stretch in the *O*-protonated product (calcd 3597 cm^{-1}) than the N–H stretch in the *N*-protonated reactant (calcd 2721 cm^{-1}), see the Supporting Information

22. Hart PJ, Balbirnie MM, Ogihara NL, Nersissian AM, Weiss MS, Valentine JS, Eisenberg D. Biochemistry. 1999; 38:2167–2178. [PubMed: 10026301]

23. Helm ML, Stewart MP, Bullock RM, DuBois MR, DuBois DL. Science. 2011; 333:863–866. [PubMed: 21836012]

A) Rational ligand design

B) n-TMC/M/O$_2$ Species

C) End-on ^{E}P Cu$_2$O$_2$ complexes

(^{E}P) [(TMPA)$_2$Cu^{II}$_2$(O$_2$$^{2-}$)]$^{2+}$ (^{E}P) [(*tetb*)$_2$Cu^{II}$_2$(O$_2$$^{2-}$)]$^{2+}$
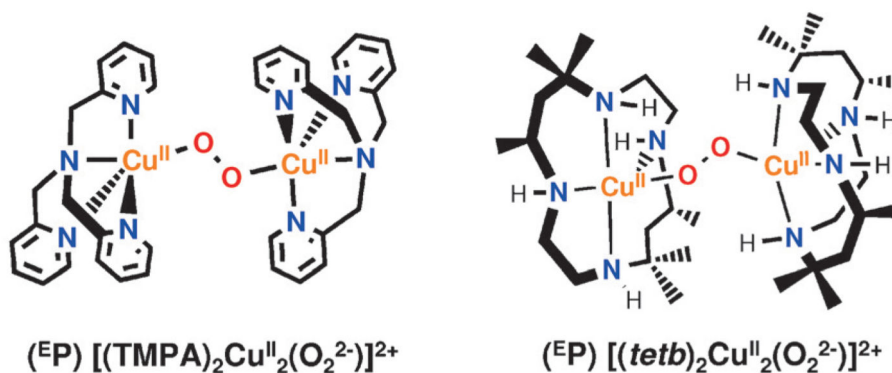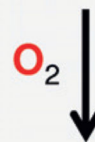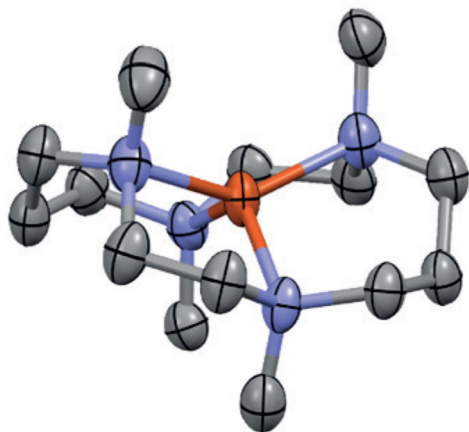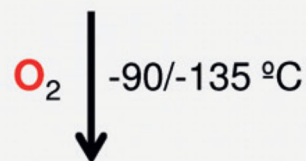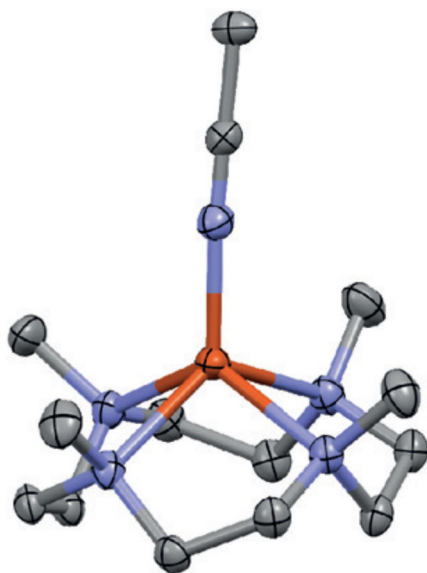
Figure 1.
Controlled generation of different LCu–O$_2$ species by rational ligand design A) First row metal/O$_2$ species bearing macrocyclic 14-TMC and 12-TMC ligands. B) Crystallographically characterized ^{E}**P** species (C).[5a,10]

A) *TV*-[(14-TMC)**Cu**^{I}](BAr^F)

TV-[(**14-TMC**)**Cu**^{I}]$^+$

O$_2$ $\downarrow$

No reaction

B) *TI*-[(12-TMC)**Cu**^{I}(CH$_3$CN)](BAr^F)

TI-[(**12-TMC**)**Cu**^{I}(CH$_3$CN)]$^+$

O$_2$ $\downarrow$ -90/-135 ºC

Green CuO$_2$ species

Figure 2.
Displacement ellipsoid plots (50% probability level) of *TV*-[(14-TMC)Cu^I]$^+$. A) (un-reactive towards O$_2$) and *TI*-[(12-TMC)Cu^I(CH$_3$CN)]$^+$ B) (reactive with O$_2$). For clarity, the BAr^F anions and the H atoms are not depicted. See the Supporting Information for synthetic details and structural features.
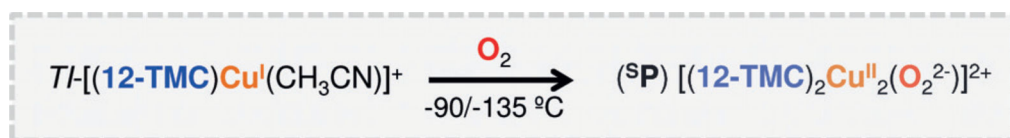
Figure 3.
A) Spectroscopic characterization (UV/Vis) of green [(12-TMC)$_2$Cu$^{II}_2$(O$_2^{2-}$)]$^{2+}$ (λ_{max} = 364 nm) generated by the oxygenation of *Tl*-[(12-TMC)Cu^I(CH$_3$CN)]$^+$. Inset: rR spectra (λ = 380 nm) of [(12-TMC)$_2$Cu$^{II}_2$(O$_2^{2-}$)]$^{2+}$ generated from ^{16}O$_2$ and ^{18}O$_2$ (*), and ^{16}O$_2$–^{18}O$_2$ subtraction. B) DFT optimized structure of ^{S}P [(12-TMC)$_2$Cu$^{II}_2$(O$_2^{2-}$)]$^{2+}$ and TD-DFT calculated spectroscopic features (rR and UV/Vis).

A) *Reactivity of Cu$_2$O$_2$ cores compared to* (^{S}P) [(12-TMC)$_2$Cu$^{II}_2$(O$_2^{2-}$)]$^{2+}$
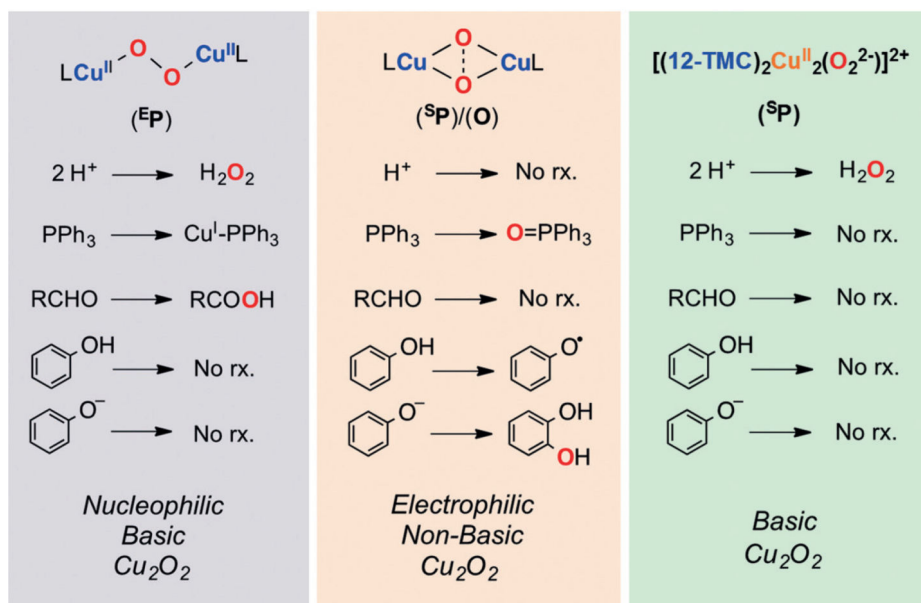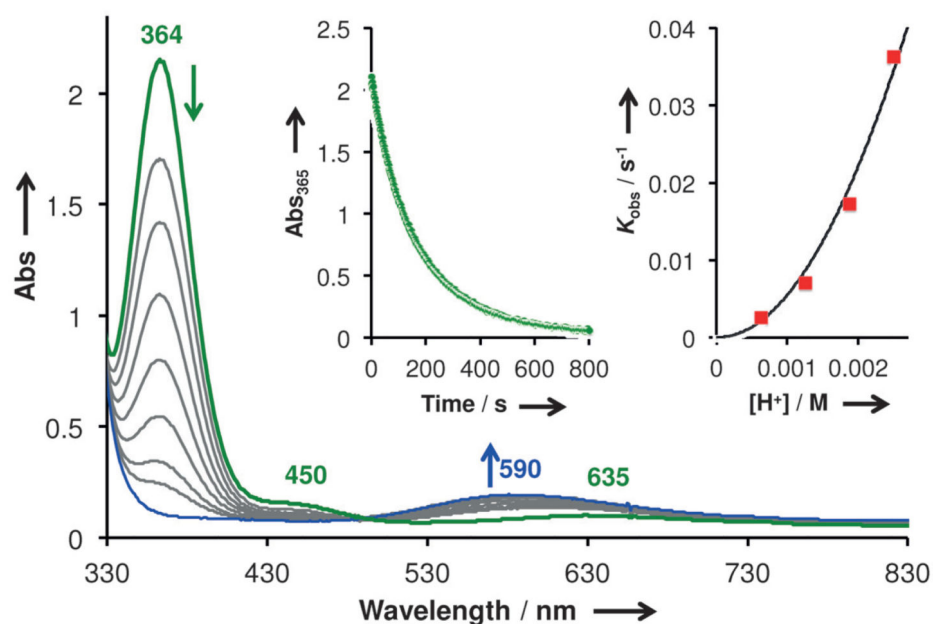
Figure 4.
A) Reactivity towards external substrates shown by ^{S}**P** [(12-TMC)$_2$Cu$^{II}_2$(O$_2^{2-}$)]$^{2+}$ (right) compared to generic reactivity of ^{E}**P** and ^{S}**P/O** cores. B) UV/Vis changes and kinetic analysis (inset) for the reaction of [(12-TMC)$_2$Cu$^{II}_2$(O$_2^{2-}$)]$^{2+}$ (λ_{max} = 364 nm) with acid to generate 2 equivalents of [(12-TMC)Cu^{II}]$^{2+}$ (λ_{max} = 590 nm) and H$_2$O$_2$.
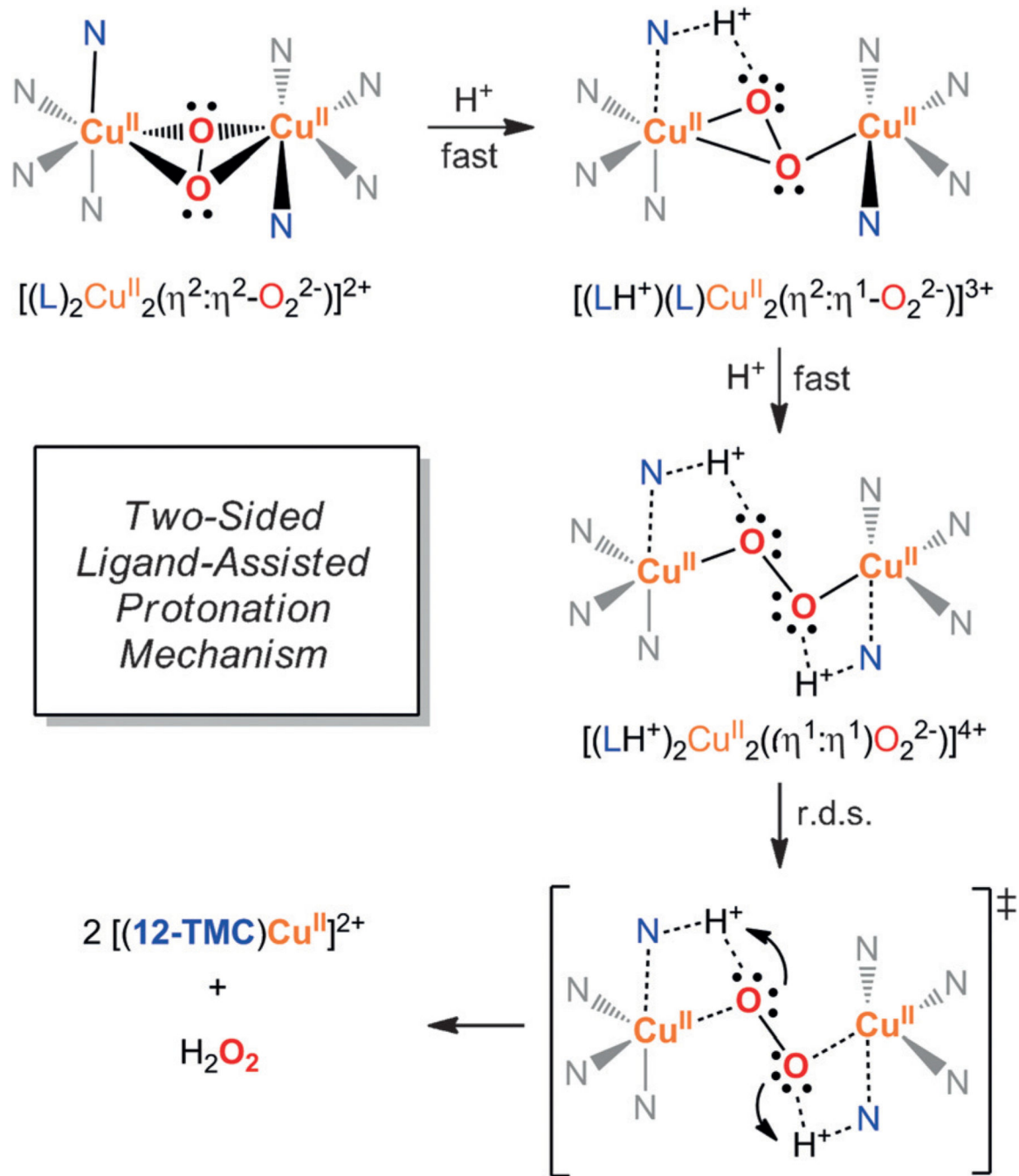
Figure 5.
Proposed reaction mechanism for the protonation of $[(12\text{-}TMC)_2Cu^{II}_2(O_2^{2-})]^{2+}$ based on experimental findings and DFT calculations.